

Optimal multiyear management of a water supply system under uncertainty: Robust counterpart approach

Mashor Housh,¹ Avi Ostfeld,¹ and Uri Shamir¹

Received 24 February 2011; revised 29 July 2011; accepted 29 August 2011; published 15 October 2011.

[1] In this paper, the robust counterpart (RC) approach (Ben-Tal et al., 2009) is applied to optimize management of a water supply system (WSS) fed from aquifers and desalination plants. The water is conveyed through a network to meet desired consumptions, where the aquifers recharges are uncertain. The objective is to minimize the net present value cost of multiyear operation, satisfying operational and physical constraints. The RC is a min-max guided approach, which converts the original problem into a deterministic equivalent problem, requiring only that the uncertain parameters resides within a user-defined uncertainty set. The robust policy obtained by the RC approach is compared with policies obtained by other decision-making approaches including stochastic approaches.

Citation: Housh, M., A. Ostfeld, and U. Shamir (2011), Optimal multiyear management of a water supply system under uncertainty: Robust counterpart approach, *Water Resour. Res.*, 47, W10515, doi:10.1029/2011WR010596.

1. Introduction

[2] Optimal planning and management of water supply systems (WSS) has been studied extensively and resulted in many optimization models and techniques. The parameters of early models were usually assumed perfectly known, leading to deterministic models. The results obtained by such models may perform poorly when implemented in the real world, when the problem parameters are revealed and differ from those assumed in the deterministic model.

[3] There are approaches that handle uncertainty in the problem parameters, notably stochastic programming. A variety of stochastic methods have been applied to WSS management, including stochastic dynamic programming [Yeh, 1985; Faber and Stedinger, 2001], implicit stochastic optimization [Lund and Ferreira, 1996; Labadie, 2004], scenarios-based optimization [Pallottino et al., 2005; Kracman et al., 2006], and chance constraint methods [Lansley et al., 1989; Sankarasubramanian et al., 2009]. In these stochastic programming methods the uncertain data are assumed to have a known probability density function (PDF). A drawback is that the PDF itself must be recognized as being uncertain.

[4] In classical stochastic programming the models are designed to minimize the expected value of a cost function or maximize a net benefit function, and do not facilitate evaluation of the trade-offs between the risks of infeasibility and the losses in optimality.

[5] Robust optimization (RO) is a framework for incorporating risk aversion into optimization models and finding robust solutions. One can distinguish between probabilistic and nonprobabilistic RO methods. Modern RO deals primarily with nonprobabilistic models of robustness. The term “robust optimization” is used quite frequently in the

literature, while researchers often do not distinguish between probabilistic and nonprobabilistic RO when they use the descriptor “robust” in their papers’ titles, even if in the paper body it can be discerned which version they use. Therefore, the specific meaning and implications of RO have become somewhat elusive.

[6] The probabilistic RO is attributed to *Mulvey et al.* [1995], which is also known as scenario-based RO. *Mulvey et al.* [1995] used the slack variables of soft constraints to penalize the objective function when soft constraints are violated. Higher moments (e.g., variance) were then introduced into the objective function as a measure of risk. For instance, if the variance is used (as in the case of the original *Mulvey et al.*’s [1995] paper), the scenario-based RO allows the evaluation of trade-offs between the expected value of the objective function, the variability in the value of the objective function, and the risk of violating soft constraints.

[7] Various applications of this scenario-based RO were reported in the past decade [*Watkins and McKinney*, 1997; *Escudero*, 2000; *Jia and Culver*, 2006]. In *Watkins and McKinney* [1997] the new RO (at that time) methodology proposed by *Mulvey et al.* [1995] was applied to an urban water management problem, where they seek solutions that hedge against inherent parameter uncertainty by using the scenario-based RO.

[8] It is instructive to note that the scenario-based RO shares a number of disadvantages with stochastic programming: (a) data: uncertain data are assumed to have a known PDF, which in reality is itself uncertain; (b) structure: how to build a “representative” sample of scenarios, using the PDFs?; (c) tractability: to represent the PDF support, a large sample of scenarios is usually needed, which can be very difficult to process computationally. *Watkins and McKinney* [1997] state “One disadvantage of RO is the potential size and complexity of the resulting model. As a result, special solution algorithms may be required.”

[9] Beyond the disadvantages of the scenario-based RO raised above, some researchers demonstrate conceptual

¹Faculty of Civil and Environmental Engineering, Technion, Israel Institute of Technology, Haifa, Israel.

concerns regarding *Mulvey et al.*'s [1995] approach. *Sen and Hgle* [1999] state "the RO model paints a misleading picture of the variance of the second-stage objective" and fortify their claim by a numerical example.

[10] More than a decade ago, a new nonprobabilistic RO method, the robust counterpart (RC) approach, was proposed [*Ben-Tal and Nemirovski*, 1999; *Bertsimas and Sim*, 2004] and used in a number of applications which includes portfolio models [*Ben-Tal et al.*, 2000b; *Lobo and Boyd*, 2000], inventory theory [*Bertsimas and Thiele*, 2006; *Bienstock and Ozbay*, 2008], process scheduling [*Li and Ierapetritou*, 2008], and network models [*Mudchanatongsuk et al.*, 2005].

[11] The RC approach is a novel method for optimization under uncertainty, in which the uncertainty is not described by a PDF or scenarios, but is rather "deterministic" [*Ben-Tal and Nemirovski*, 1999] which is known to reside within a user-defined uncertainty set. Hence, instead of immunizing the solution in a probabilistic sense, the decision-maker searches for a solution that is optimal for all possible realizations of the uncertainty set.

[12] The RC approach developed by *Ben-Tal and Nemirovski* [1999] considers ellipsoidal uncertainty sets while the RC approach suggested by *Bertsimas and Sim* [2004] considers polyhedral uncertainty sets. Both approaches have advantages and disadvantages. In the RC [*Ben-Tal and Nemirovski*, 1999] the use of the ellipsoidal uncertainty set can be probabilistically justified (section 2.2 below) and the resulting RC has the same size as the original model, while the size of the polyhedral RC [*Bertsimas and Sim*, 2004] increases. On the other hand, the polyhedral RC is linear like the original problem, while the ellipsoidal RC results in second-order nonlinear cone programming.

[13] For the WSS problem we use the ellipsoidal RC as we prove (section 4.2) that the RC obtained is linear programmed (LP) with the same size as the original problem and therefore has clear preference. For numerical comparison between the two approaches the reader is referred to *Li and Ierapetritou* [2008, p. 4153]. For an application of the polyhedral RC [*Bertsimas and Sim*, 2004] the reader is referred to *Chung et al.* [2009] for an application to WSS design under demand uncertainty.

[14] Section 2 presents the basics of the RC method. Section 3 presents formulation of the WSS model, its objective function and constraints. Section 4 describes the application of the RC to the WSS model, namely structuring the model for the optimization solver. Section 5 presents applications of the RC to two WSS models.

2. Robust Counterpart (RC) Approach

[15] The RC approach is a min-max-oriented method [*Ben-Tal and Nemirovski*, 1998, 2000a] that seeks robust feasible/optimal "here and now" decisions which are determined at the beginning of the time horizon, before the uncertain data are revealed. This version of the RC approach is termed the "static problem."

[16] Robust feasible decisions treat the uncertain constraints as hard constraints, i.e., constraints which have to be satisfied for all realizations within the given uncertainty set, while robust optimal means optimizing the guaranteed value (for a minimization problem it is the largest value) of the objective function over the uncertainty set.

[17] The RC approach is flexible enough to allow treating soft constraints in which feasibility is not essential, such as demand constraints, when water users can accept minor water shortages with an associated cost (penalty). *Mulvey et al.* [1995] used the slack variables of soft constraints to penalize the objective function when soft constraints are violated. Introducing slack variables in soft constraints converts them to hard constraints which must remain feasible for all realizations of the uncertainty set.

[18] The RC can also allow different ways to handle the objective function; for example, one can use the nominal values of the uncertain data in the objective while the constraints have to satisfy all the realization in the uncertainty set.

[19] The RC solves a *static problem* in which the decisions for all future stages are determined "here and now." As a consequence, decisions for the first stage, which are to be implemented immediately, are influenced by future information as known or forecasted at present, including: planned or already committed modifications of the supply system, future cost figures, forecasted demands, and hydrological forecasts. In practice, the model will be run again at the end of the first stage with whatever information has been added or updated and starting with the actual state of the supply system at that time. This process is captured by the "folding RC" approach (FRC) [*Ben-Tal et al.*, 2000b] addressed in section 5.3.

2.1. Robust Counterpart of an Uncertain Linear Program

[20] Consider the following problem subject to data uncertainty:

$$\min_y \{c_0^T y : A_0 y \leq b_0\}. \quad (1)$$

[21] We assume without any loss of generality that the data uncertainty only affects the elements in the coefficient matrix. If there is uncertainty in the objective or in the right-hand side (RHS), we can rewrite the linear programming (LP) problem as

$$\min_x \{c^T x : Ax \leq 0\}, \quad (2)$$

where $x = [z, y, 1]^T$ (the last element is 1 to represent the RHS); $A = \begin{pmatrix} -1 & c_0^T & 0 \\ 0 & A_0 & -b_0 \end{pmatrix}$ and $c = [1, 0, \dots, 0]^T$.

[22] The RC of problem (2) is

$$\min_x \{c^T x : Ax \leq 0, \forall A \in U\}, \quad (3)$$

where U is a user-defined uncertainty set. According to *Ben-Tal et al.* [2009, p. 11], an LP with a certain objective is a constraintwise problem, i.e., the RC solution does not change if the uncertainty set is extended to the product of its projections on the subspaces of the constraints, i.e., instead of solving (3) one can solve:

$$\min_x \{c^T x : a_i^T x \leq 0, \forall i, \forall a_i \in U_i\}, \quad (4)$$

where a_i^T is row i in matrix A and U_i is the projection of U on the space of the data of a_i .

[23] Worst case-oriented methods often lead to overly conservative solutions such as *Soyster's* [1973] which considers interval and columnwise uncertainties in LP, where every uncertain parameter takes its worst-case value in the uncertainty set. To address over-conservativeness, the RO method introduces ellipsoidal uncertainty sets to reflect the fact that the coefficients of the constraints are not expected to be simultaneously at their worst values.

[24] The ellipsoidal uncertainty set is defined as affine mapping of a ball of radius θ :

$$U_i = \{a_i : \hat{a}_i + \Delta\varsigma, \|\varsigma\| \leq \theta\}, \quad (5)$$

where \hat{a}_i is the nominal value, Δ is the mapping matrix, and the parameter θ is a subjective value chosen by the decision-maker to reflect his attitude toward risk. *Ben-Tal et al.* [1999] show that the RC of the LP constraints is

$$\begin{aligned} & a_i^T x \leq 0 \quad \forall a_i \in \{\hat{a}_i + \Delta\varsigma, \|\varsigma\| \leq \theta\} \\ & \Leftrightarrow \\ & \max_{\|\varsigma\| \leq \theta} [\hat{a}_i^T x + (\Delta\varsigma)^T x] \leq 0 \\ & \Leftrightarrow \\ & \hat{a}_i^T x + \theta \|x^T \Delta\| \leq 0, \end{aligned} \quad (6)$$

which is a convex tractable optimization problem that can be solved by polynomial time interior point algorithms. When only some of the parameters are uncertain, e.g., a_{i1} is a vector of certain parameters and a_{i2} a vector of uncertain parameters in row i of the matrix A , the RC is

$$\begin{aligned} & a_{i1}^T x_1 + a_{i2}^T x_2 \leq 0 \quad \forall a_{i2} \in \{\hat{a}_{i2} + \Delta_2\varsigma_2, \|\varsigma_2\| \leq \theta\} \\ & \Leftrightarrow \\ & a_{i1}^T x_1 + \hat{a}_{i2}^T x_2 + \theta \|x_2^T \Delta_2\| \leq 0, \end{aligned} \quad (7)$$

where x_1, x_2 are the elements of x corresponding to a_{i1}, a_{i2} , respectively. A special case is when the only uncertainty is on the right-hand side, in vector b_0 . In this case $x = [z, y, 1]^T$ from (2) is separated into $x_1 = [z, y]^T$ and $x_2 = 1$; hence, we obtain a linear RC of the form

$$a_{i1}^T x_1 + \hat{a}_{i2}^T + \theta \|\Delta_2\| \leq 0. \quad (8)$$

2.2. Why Ellipsoidal Uncertainty?

[25] Several considerations lead to the selection of an ellipsoidal uncertainty set: (1) it leads to an explicit convex tractable RC which can be solved by polynomial time methods such as interior-point. (2) ellipsoidal uncertainty is defined by the subjective safety parameter θ , which allows the decision-maker to solve the robust counterparts of the problem for different values of θ , and thereby obtain the tradeoff between robustness and performance. (3) Using an ellipsoidal uncertainty set can be stochastically justified, even though no underlying PDF is assumed to be known for the uncertain parameters.

[26] Partial information on the uncertain data is often available and can be used in defining the ellipsoid. Simple probabilistic arguments such as first and second moments

of the stochastic parameters (expectation and variance) can be used to replace stochastic uncertainty by an ellipsoidal deterministic uncertainty. To demonstrate this let us consider the linear constraint:

$$a_1^T x_1 + a_2^T x_2 \leq 0, \quad (9)$$

where a_2 is random vector with expectation vector μ_{a_2} and covariance matrix Σ_{a_2} . Thus, the left-hand side of the constraint is a stochastic random variable with expectation μ_l , and variance Σ_l defined as

$$\mu_l = E[a_1^T x_1 + a_2^T x_2] = a_1^T x_1 + \mu_{a_2}^T x_2, \quad (10)$$

$$\Sigma_l = \text{Var}[a_1^T x_1 + a_2^T x_2] = x_2^T \Sigma_{a_2} x_2 = x_2^T \Delta \Delta^T x_2 = \|x_2^T \Delta\|^2, \quad (11)$$

where $\Sigma_{a_2} = \Delta \Delta^T$. The matrix Δ can be obtained by the Cholesky decomposition. If we define the ‘‘safe’’ version of the constraint as the realization of the stochastic left side when deviated by θ standard deviations, we obtain:

$$\begin{aligned} & \mu_l + \theta \|x_2^T \Delta\| \leq 0 \\ & a_1^T x_1 + \mu_{a_2}^T x_2 + \theta \|x_2^T \Delta\| \leq 0, \end{aligned} \quad (12)$$

which is the same as the robust counterpart with ellipsoidal uncertainty set:

$$U_{a_2} = \{a_2 = \mu_{a_2} + \Delta\varsigma, \|\varsigma\| \leq \theta\}. \quad (13)$$

[27] Hence, if we solve the linear robust counterpart in which the coefficients belong to the ellipsoidal uncertainty set defined above, it is the same as saying that we are immunized against θ standard deviations of the constraint.

[28] Note that the stochastic vector a_2 , with expectation μ_{a_2} and covariance matrix Σ_{a_2} , can be described as an affine transformation of the random vector ξ with expectation $\mu_\xi = 0$ and covariance matrix $\Sigma_\xi = I$:

$$a_2 = \mu_{a_2} + \Delta\xi, \quad (14)$$

since $\mu_{a_2} = \mu_{a_2} + \Delta\mu_\xi = \mu_{a_2}$ and $\Sigma_{a_2} = \Delta\Sigma_\xi\Delta^T = \Delta\Delta^T$.

[29] Thus, the construction of the ellipsoidal uncertainty set replaces the stochastic variables ξ by the perturbation vector ς varying in the perturbation set $\text{Ball}_\theta = \{\|\varsigma\| \leq \theta\}$.

3. Management Model of a Water Supply System (WSS)

[30] We consider management of a WSS where water is taken from sources, conveyed through a conveyance, and distribution network to consumers. Mathematical optimization models have proven their usefulness in dealing with such problems [*Loucks et al.*, 1981]. Various types of models can be applied to WSS, depending on the time horizon and time steps, ranging from long-term development of large systems, to detailed operation of smaller parts. Thus, models range from highly aggregate versions of an entire water system to much more detailed models in space and

time [Shamir, 1971]. The short-term (weekly to annual) or long-term (years, decades) operation of a large-scale water supply system can be captured in a model of medium aggregation that is used to simultaneously manage water sources, water demands, and the network [Fisher et al., 2002; Draper et al., 2003, 2004; Jenkins et al., 2004; Watkins et al., 2004; Zaide, 2006].

[31] Here we consider an optimization model with a medium aggregation level: water is taken from sources, which include aquifers, reservoirs, and desalination plants, conveyed through a distribution system to consumers who require certain quantities of water, see Figure 1 (small system, for which we provide detailed analysis) and Figure 7 (large system, only major results). The time horizon covers several years, with an annual time step. The operation is subject to constraints such as water levels in the aquifers, capacities of the pumping stations, carrying capacities of the distribution system, and production capacity of the desalination plants. The objective is to operate the system with a minimum total cost of desalination and pumping, plus a depletion penalty for ending below a prescribed final level in the aquifers, which becomes a reward if the final state is higher than this level.

[32] The network representation in the model can be classified according to the physical laws that are considered explicitly in the model constraints [Ostfeld and Shamir, 1993; Cohen et al., 2000]. According to this classification, the proposed model is a flow model, which only considers the balance of flows without explicit inclusion of the hydraulics. The inherent assumption of this flow model is that the detailed hydraulic operation of the system to deliver the quantities prescribed by the model is feasible. A further consideration included in the proposed model is sustainability of the management plan. This implies meeting the needs of the present without reducing the ability of the next generation to meet its needs [Loucks, 2000]. This is represented by a relatively long time-horizon with specified state conditions at its end. An allied aspect of multiyear WSS management relates to hydrological uncertainty [Ajami et al., 2008], climate change [Brekke et al., 2009; Yates et al., 2005], population growth [Kasprzyk et al., 2009], and the decline of water quality in the sources.

However, in the current paper only the replenishment into the natural resources is taken as uncertain.

3.1. Mathematical Model

3.1.1. Objective Function

[33] The objective is to operate the system with minimum total cost composed of desalination and conveyance costs over the operation horizon T_f years, and a penalty/reward related to the final state of the aquifers at the end of the planning horizon. This term depends on the deviation of the final water level from a prescribed value: being below it incurs a penalty while being above it results in a reward. Henceforth, all values are in million cubic meters per year (MCM/yr) and the costs are in (\$/MCM), where $a, d, l, z,$ and t denote aquifer, desalination, link, demand zone, and year, respectively. The objective is

$$\sum_{t=1}^{T_f} \left[\sum_d des_{d,t} Q_{d,t} + \sum_l C_{l,t} Q_{l,t} \right] + \sum_a \left[(\hat{h}_a - h_{a,T_f}) E_a \right] \rightarrow \min, \tag{15}$$

where $des_{d,t}$ is the cost of desalinated water per MCM (\$/MCM); $Q_{d,t}$ is the desalinated water amount (MCM/yr); $C_{l,t}$ is the cost of transportation per MCM (\$/MCM); $Q_{l,t}$ is the flow in the link (MCM/yr); $h_{a,t}$ is the water level (m) in the aquifer at the end of year t ; \hat{h}_a is the prescribed final water level (m); and E_a is penalty per unit deviation (\$/m).

3.1.2. Constraints

3.1.2.1. Water Conservation Law

[34] The distribution system is represented as a directed graph consisting of N nodes connected by M edges. The nodes can be grouped into two subgroups: N_1 are source nodes, desalination plant, and aquifers, with one outgoing link from each source node; and N_2 intermediate and demand nodes, where two or more edges meet. The M edges represent the links between two nodes; links in which the direction of flow is not fixed are represented by two edges, one in each direction. The topology of the network is represented by the junction node connectivity matrix G , where $G \in \mathbf{R}^{N_2 \times M}$ has a row for each node and a column for each edge. The

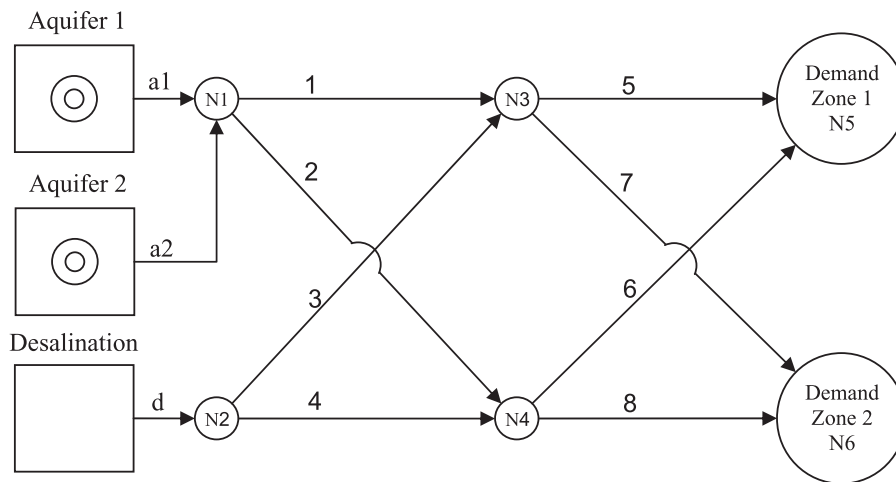


Figure 1. Network layout.

nonzero elements in each row are +1 and -1 for incoming and outgoing edges, respectively. The first columns in G correspond to the links, which leave source nodes (aquifers and desalination plants), while the last rows correspond to the demand nodes. For each year t , the following linear equation system insures water conservation at the network nodes:

$$GQ_t = S_t, \tag{16}$$

where $Q_t = [Q_{\text{natural},t}, Q_{\text{desalination},t}, Q_{\text{links},t}]^T$; $S_t = [0, Q_{\text{demand},t}]^T$; $Q_{\text{natural},t}$ is the vector of elements $Q_{a,t} \forall a$; $Q_{\text{desalination},t}$ is the vector of elements $Q_{d,t} \forall d$; $Q_{\text{links},t}$ is the vector of elements $Q_{l,t} \forall l$; $Q_{\text{demand},t}$ is the vector of elements $Q_{z,t} \forall z$ where $Q_{z,t}$ denotes demand at year t in demand zone z . The water supply network shown in Figure 1 has three source nodes, four intermediate nodes, and two demand nodes. The junction node connectivity matrix $G \in R^{6 \times 11}$ is given in Table 1. The vectors Q_t, S_t are: $Q_t = [Q_{a,t}, Q_{d,t}, Q_{l,t}, \dots, Q_{8,t}]^T$ and $S_t = [0, \dots, 0, Q_{z=1,t}, Q_{z=2,t}]^T$.

3.1.2.2. Hydrological Balance for Aquifers

[35] The hydrological water balance insures that the change in aquifer storage equals the difference between the recharge and withdrawal during the year:

$$h_{a,t} = h_{a,0} + \frac{1}{SA_a} \left(\sum_{i=1}^t R_{a,i} - \sum_{i=1}^t Q_{a,i} \right), \tag{17}$$

where $Q_{a,t}$ is the extraction amount (MCM/yr); $R_{a,t}$ is recharge (MCM/yr); SA_a is the storativity multiplied by area (MCM/m); $h_{a,t}$ is the water level in the aquifer at the end of year t (m); and $h_{a,0}$ is the initial water level (m).

3.1.2.3. Limits on Water Levels in the Sources

[36] Constraints on water levels in the natural resources reflect both policy and physical/operational limits:

$$h_{a,t}^{\min} \leq h_{a,t} \leq h_{a,t}^{\max}, \tag{18}$$

where $h_{a,t}^{\min}$ is the minimum allowed water level (m); $h_{a,t}^{\max}$ is the maximum allowed water level (m).

3.1.2.4. Conveyance Capacity Constraints

[37] The model deals with water balance and does not explicitly include the hydraulic energy equations. Still, to maintain feasibility of hydraulic conditions the discharges in the links are limited by capacity constraints, which are calculated from the hydraulic data of the pipes/links. The lower bound is set to zero since the flow direction in the links is fixed:

$$0 \leq Q_{l,t} \leq Q_{l,t}^{\max}, \tag{19}$$

where $Q_{l,t}^{\max}$ is the maximum discharge allowed (MCM/yr).

Table 1. The Junction Node Connectivity Matrix for the Network in Figure 1

| Node | Source | | | Links | | | | | | | |
|------|--------|----|---|-------|----|----|----|----|----|----|----|
| | a1 | a2 | d | 1 | 2 | 3 | 4 | 5 | 6 | 7 | 8 |
| 1 | 1 | 1 | 0 | -1 | -1 | 0 | 0 | 0 | 0 | 0 | 0 |
| 2 | 0 | 0 | 1 | 0 | 0 | -1 | -1 | 0 | 0 | 0 | 0 |
| 3 | 0 | 0 | 0 | 1 | 0 | 1 | 0 | -1 | 0 | -1 | 0 |
| 4 | 0 | 0 | 0 | 0 | 1 | 0 | 1 | 0 | -1 | 0 | -1 |
| 5 | 0 | 0 | 0 | 0 | 0 | 0 | 0 | 1 | 1 | 0 | 0 |
| 6 | 0 | 0 | 0 | 0 | 0 | 0 | 0 | 0 | 0 | 1 | 1 |

3.1.2.5. Capacities of Natural Sources

[38] The extracted amount from each natural resource may be restricted by an upper bound, reflecting various hydrological and hydraulic considerations. The lower bound is set to zero as the flow from the source is one-directional:

$$0 \leq Q_{a,t} \leq Q_{a,t}^{\max}, \tag{20}$$

where $Q_{a,t}^{\max}$ is the maximum admissible/feasible withdrawal (MCM/yr).

3.1.2.6. Desalination Capacity

[39] The amount of desalinated water from each plant is limited by an upper bound which represents plant capacity and by a lower bound that represents a condition usually set in the contract with the plant owners (which may be zero):

$$Q_{d,t}^{\min} \leq Q_{d,t} \leq Q_{d,t}^{\max}, \tag{21}$$

where $Q_{d,t}^{\max}$ is maximum supply (MCM/yr); and $Q_{d,t}^{\min}$ is minimum supply (MCM/yr).

[40] The resulting mathematical model is an uncertain LP where the uncertainty is in the recharge parameters $R_{a,t} \forall a \forall t$. Hence, we can define the uncertain column vector $R = [R_{a=1..a_f,t=1}, \dots, R_{a=1..a_f,t=T}]^T$, where a_f is the number of natural resources.

4. Applying the RC Approach

4.1. Constructing the Uncertainty Set

[41] Recharge into natural resources is usually given as a historical time series, frequently of limited duration, and sometimes not rich enough to adequately describe the stochastic process. To construct an ellipsoidal uncertainty set for the natural resources recharge, we assume that the annual recharge values are independent random variables, where the recharge vector of the aquifers $R^t = R_{a=1..a_f,t}$ in each year t is correlated with covariance matrix Σ_{R^t} and expectation vector μ_{R^t} , indicating positive correlation between the recharge of different aquifers (e.g., a wet year is wet all over). Each row in Σ_{R^t} and μ_{R^t} corresponds to an aquifer $a = 1..a_f$. The annual recharges are assumed independent over time so the recharge data is repeated for the entire horizon. Hence, the expectation vector of the overall recharge is $\mu_R = [\mu_{R^1}, \dots, \mu_{R^T}]^T$ and covariance matrix Σ_R is a diagonal block matrix:

$$\Sigma_R = \begin{pmatrix} \Sigma_{R^1} & 0 & 0 \\ 0 & \ddots & 0 \\ 0 & 0 & \Sigma_{R^T} \end{pmatrix}. \tag{22}$$

[42] Consider the linear transformation of the stochastic vector R :

$$\begin{aligned} R &= \mu_R + \Delta \xi, \\ \mu_R &= \mu_R + \Delta \mu_\xi, \\ \Sigma_R &= \Delta \Sigma_\xi \Delta^T. \end{aligned} \tag{23}$$

[43] If we set $\mu_\xi = 0$ and $\Sigma_\xi = I$ and we wish to maintain the covariance of R , then $\Sigma_R = \Delta \Delta^T$. By replacing the stochastic vector ξ with the perturbation vector ς that

varies in the perturbation set $\text{Ball}_\theta = \{\|\zeta\| \leq \theta\}$, we obtain the ellipsoidal uncertainty set U of the uncertain vector R :

$$U = \{R : \mu_R + \Delta\zeta, \|\zeta\| \leq \theta\}. \quad (24)$$

[44] The parameter θ determines the range of values of the uncertain R against which the optimal policy is immunized, i.e., remains feasible. A large value means immunization against more extreme values of R . $\theta = 0$ implies that only the expected value of R is taken into consideration, and any deviation of its actual value from this expectation could lead to constraint violation.

[45] The matrix $\Delta = \sum_R^{0.5}$ can be obtained by the Cholesky decomposition. Each row in Δ corresponds to year t and aquifer a and implies $\sigma_a = \|\Delta_{t,a}\|$, where σ_a is the standard deviation of recharge in aquifer a which remains constant over the years.

4.2. Formulation of the RC

[46] Formulation of a RC for the WSS model developed in section 3 requires extracting the state variable $h_{a,t}$ from the uncertain equation (17). The resulting model, after substituting $h_{a,t}$ and converting it to the form of the LP in (2) is

$$K \rightarrow \min$$

Subject to

$$\begin{aligned} \text{(I)} \quad & \sum_{t=1}^{T_f} \sum_a \frac{E_a Q_{a,t}}{SA_a} - \sum_{t=1}^{T_f} \sum_a \frac{E_a R_{a,t}}{SA_a} + \sum_{t=1}^{T_f} \sum_d des_{d,t} Q_{d,t} \\ & + \sum_{t=1}^{T_f} \sum_l C_{l,t} Q_{l,t} + P_0 - K \leq 0, \\ \text{(II)} \quad & \begin{cases} h_{a,0} + \frac{1}{SA_a} \left(\sum_{i=1}^t R_{a,i} - \sum_{i=1}^t Q_{a,i} \right) - h_{a,t}^{\max} \leq 0 & \forall a \forall t \\ -h_{a,0} - \frac{1}{SA_a} \left(\sum_{i=1}^t R_{a,i} - \sum_{i=1}^t Q_{a,i} \right) + h_{a,t}^{\min} \leq 0 & \forall a \forall t \end{cases}, \\ \text{(III)} \quad & \begin{cases} GQ_t = S_t & \forall t \\ Q_{d,t}^{\min} \leq Q_{d,t} \leq Q_{d,t}^{\max} & \forall d \forall t \\ 0 \leq Q_{a,t} \leq Q_{a,t}^{\max} & \forall a \forall t \\ 0 \leq Q_{l,t} \leq Q_{l,t}^{\max} & \forall l \forall t \end{cases} \end{aligned} \quad (25)$$

where $P_0 = \sum_a (\hat{h}_a - h_{a,0}) E_a$ is a certain constant.

[47] Consider the vectorized version of the uncertain constraints (I) and (II):

$$\begin{aligned} & \sum_{t=1}^{T_f} \sum_a \frac{E_a Q_{a,t}}{SA_a} - R^T D_{SA}^{-1} v + \sum_{t=1}^{T_f} \sum_d des_{d,t} Q_{d,t} \\ & + \sum_{t=1}^{T_f} \sum_l C_{l,t} Q_{l,t} + P_0 - K \leq 0 \\ & h_{a,0} + R^T D_{SA}^{-1} \delta_{a,t} - \frac{1}{SA_a} \sum_{i=1}^t Q_{a,i} - h_{a,t}^{\max} \leq 0 \quad \forall a \forall t \\ & -h_{a,0} - R^T D_{SA}^{-1} \delta_{a,t} + \frac{1}{SA_a} \sum_{i=1}^t Q_{a,i} + h_{a,t}^{\min} \leq 0 \quad \forall a \forall t, \end{aligned} \quad (26)$$

where $R = [R_{a=1..a_f, t=1}, \dots, R_{a=1..a_f, t=T_f}]^T$; $v = [E_{a=1..a_f}, \dots, E_{a=1..a_f}]^T$; $\delta_{a,t} \in \mathbf{R}^{(a_f \times T_f \times 1)}$ has 0 and 1 values according to a, t , in order to extract the elements corresponding to the constraint from the elements of R ; D_{SA} is a diagonal matrix with main diagonal vector $[SA_{a=1..a_f}, \dots, SA_{a=1..a_f}]^T \in \mathbf{R}^{(a_f \times T_f \times 1)}$. For example, when there are two aquifers, $\delta_{a=1, t=2} = [1, 0, 1, 0, 0, \dots, 0]^T$.

[48] The robust version of the uncertain constraint is (see section 2.1)

$$\begin{aligned} & \sum_{t=1}^{T_f} \sum_a \frac{E_a Q_{a,t}}{SA_a} - \mu_R^T D_{SA}^{-1} v + \theta \|v^T D_{SA}^{-1} \Delta\| \\ & + \sum_{t=1}^{T_f} \sum_d des_{d,t} Q_{d,t} + \sum_{t=1}^{T_f} \sum_l C_{l,t} Q_{l,t} + P_0 - K \leq 0 \\ & h_{a,0} + \mu_R^T D_{SA}^{-1} \delta_{a,t} + \theta \|\delta_{a,t}^T D_{SA}^{-1} \Delta\| - \frac{1}{SA_a} \sum_{i=1}^t Q_{a,i} \\ & - h_{a,t}^{\max} \leq 0 \quad \forall a \forall t \\ & -h_{a,0} - \mu_R^T D_{SA}^{-1} \delta_{a,t} + \theta \|\delta_{a,t}^T D_{SA}^{-1} \Delta\| + \frac{1}{SA_a} \sum_{i=1}^t Q_{a,i} \\ & + h_{a,t}^{\min} \leq 0 \quad \forall a \forall t. \end{aligned} \quad (27)$$

[49] The resulting RC is LP, since no decision variables appear in the norms and the uncertainty appears only on the RHS. Recalling that the data in μ_R and Δ are repeated each year and that $\sigma_a = \|\Delta_{t,a}\|$, we obtain $\mu_R^T D_{SA}^{-1} \delta_{a,t} = \frac{t \mu_{R'_a}}{SA_a}$,

$\|\delta_{a,t}^T D_{SA}^{-1} \Delta\| = \frac{\sqrt{t} \sigma_a}{SA_a}$; hence, the RC of the WSS model is

$$K \rightarrow \min$$

Subject to

$$\begin{aligned} & \sum_{t=1}^{T_f} \sum_a \frac{E_a Q_{a,t}}{SA_a} - \mu_R^T D_{SA}^{-1} v + \theta \|v^T D_{SA}^{-1} \Delta\| \\ & + \sum_{t=1}^{T_f} \sum_d des_{d,t} Q_{d,t} + \sum_{t=1}^{T_f} \sum_l C_{l,t} Q_{l,t} + P_0 - K \leq 0 \\ & h_{a,0} + \frac{t \mu_{R'_a}}{SA_a} + \theta \frac{\sqrt{t} \sigma_a}{SA_a} - \frac{1}{SA_a} \sum_{i=1}^t Q_{a,i} - h_{a,t}^{\max} \leq 0 \quad \forall a \forall t \\ & -h_{a,0} - \frac{t \mu_{R'_a}}{SA_a} + \theta \frac{\sqrt{t} \sigma_a}{SA_a} + \frac{1}{SA_a} \sum_{i=1}^t Q_{a,i} + h_{a,t}^{\min} \leq 0 \quad \forall a \forall t \\ & GQ_t = S_t \quad \forall t \\ & Q_{d,t}^{\min} \leq Q_{d,t} \leq Q_{d,t}^{\max} \quad \forall d \forall t \\ & 0 \leq Q_{a,t} \leq Q_{a,t}^{\max} \quad \forall a \forall t \\ & 0 \leq Q_{l,t} \leq Q_{l,t}^{\max} \quad \forall l \forall t. \end{aligned} \quad (28)$$

5. Examples

5.1. Problem Data

[50] A small hypothetical water supply system (Figure 1) is used for detailed demonstration. Summary results are later shown for a larger system (Figure 7) that is a central part of the Israeli National Water System. The system in

Figure 1 is fed from two aquifers and a desalination plant to supply two customers over a 10-yr horizon, for which a minimum total operation cost is sought. The annual costs of transportation in the links are $\{0.1, 0.05\}$ (M\$/MCM) for odd and even links, respectively, and the desalination cost is 1 (M\$/MCM). The same costs hold for later years $t = 2..T_f$ and are capitalized to the present (decision time) with a 5% discount rate. The penalty at the final stage is 0.3 (M\$/m) for being below the prescribed value; it becomes positive for levels above the prescribed value. Both aquifers have identical physical properties: $SA = 0.8$ (MCM/m), $h_0 = 75$ (m), $\hat{h} = 30$ (m), $h_{\min} = 0$ (m), and $h_{\max} = 500$ (m) (an arbitrary high value, to insure no spill and thus simplify the demonstration). All discharges have the same bounds: 0–100 (MCM). The annual recharges are independent and identically distributed (i.i.d.) with a joint uniform discrete distribution $\{30, 40, 50\}$ for aquifer 1 and $\{35, 50, 60\}$ for aquifer 2, respectively, and remains the same for all 10 years. This distribution implies mean recharges of $\{40, 48.33\}$ (MCM) in aquifers 1 and 2, respectively, and a covariance matrix:

$$V_{R'} = \begin{pmatrix} 66.67 & 83.33 \\ 83.33 & 105.56 \end{pmatrix}. \quad (29)$$

[51] The resulting uncertainty set of the annual recharge is

$$U = \left\{ R' : \begin{pmatrix} 40 \\ 48.33 \end{pmatrix} + \begin{pmatrix} 8.17 & 0 \\ 10.21 & 1.18 \end{pmatrix} \begin{pmatrix} s_1 \\ s_2 \end{pmatrix}, \|s\| \leq \theta \right\}. \quad (30)$$

[52] The demand in the first year is 80 (MCM) in each demand zone, and it increases by 5% in each subsequent year.

5.2. RC Solution and Simulation Results

[53] We compare five management policies: three robust policies (RP1, RP2, and RP3) obtained from the RC solution with different values of $\theta = \{1, 2, 3\}$, a nominal policy (NP) which is obtained from a deterministic solution with the average recharge, and a conservative policy (CP) which is obtained from the worst case realization, namely minimum recharge in all years. Each of these policies determines “here and now” decisions which are implemented at the beginning of the planning horizon before the uncertainty is revealed.

[54] Figure 2 compares the annual amount of desalinated water in each of these policies. The CP results in constant desalination of 120 (MCM/yr), which is the full capacity of the desalination plant. The NP takes as much as possible from the aquifers in the first stages while recognizing that demand is increasing beyond the desalination capacity which leads to storing aquifer water to close the gap between the demand and the supply capacity at later stages. The conservativeness of the CP over other policies is apparent. The robust policies RP1, RP2, and RP3 require less desalinated water than the CP, indicating that the robust policies are not myopic; in other words, they take advantage of the variability of recharge over time. Compared to the NP, a robust policy takes more desalinated water in the first stages, resulting in higher water level in the aquifers, which insures maneuverability within the operational limits of the aquifers in later years. The degree of conservativeness of the robust policies is noticeable; an RP with smaller θ results in less desalination but lower reliability/immunization and higher penalties, as will be shown below, where RP with $\theta = 0$ (which is the NP) is a lower bound.

[55] The performance of each policy is examined by simulation, which shows the tradeoff between the amount of

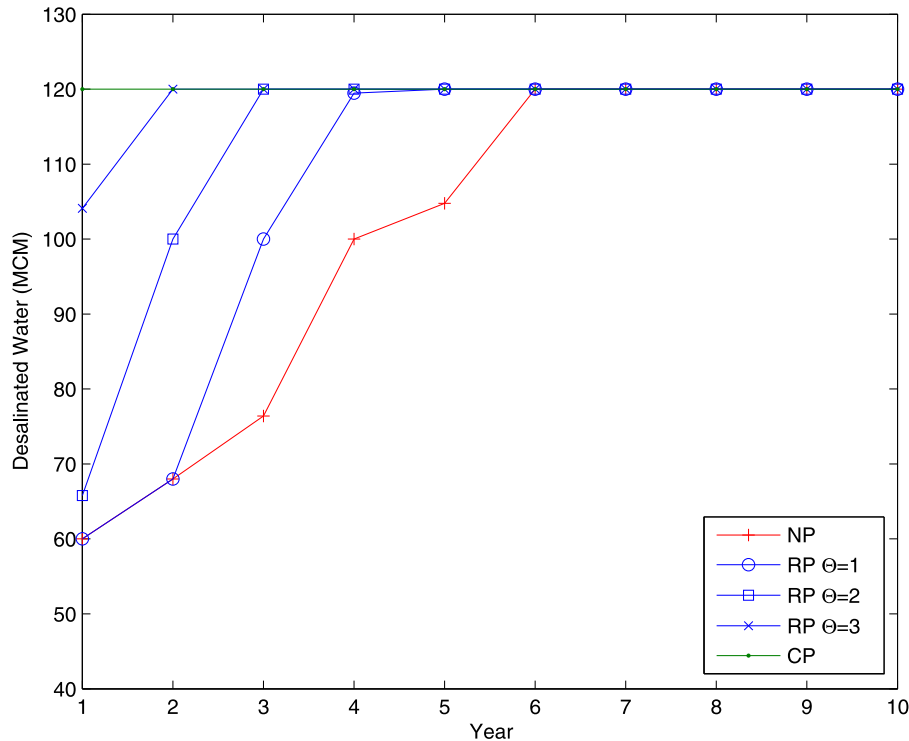


Figure 2. Desalination amount over years for each static policy.

desalination prescribed and the unreliability: lower desalination results in lower reliability. Each optimal policy is examined by simulation with 1000 random samples, each with $a_f T_f = 20$ random recharge values drawn from the defined uniform discrete distribution of the recharge. The results for NP and RP3 are shown in Figures 3 and 4, respectively: the final water levels in the two aquifers, the total cost, and the penalized cost. The feasibility of policies RP1, RP2, RP3, and NP is obviously not guaranteed for all possible realizations of the recharge, as seen by some excursions of the level to negative values. However, as seen in Figure 4 for RP3 these are very few; they are fewer as θ increases. In CP, obviously there are no infeasibilities, as it considers only the lowest value of the recharge.

[56] Since some generated samples can result in the reservoirs/aquifers becoming empty in some years, it is necessary to take this into consideration in two respects: (1) continuing the path of the reservoir/aquifer beyond this point, and (2) penalizing the policy (in this particular simulation run) for failing to meet the specified operational limits. The two aspects are handled as follows: (1) When the reservoir goes dry and “wants” to go below the minimum level, it is set back to empty as the initial state for the next year, and (2) a penalty term is added to this simulation. The penalty is

$$\max(h_{a,t}^{\min} - h_{a,t}, 0)DC_t \quad \forall a \forall t \quad (31)$$

and the water balance is

$$h_{a,t+1} = \max(h_{a,t}^{\min}, h_{a,t}) + \frac{R_{a,t+1}}{SA_a} - \frac{Q_{a,t+1}}{SA_a} \quad \forall a \forall t, \quad (32)$$

where $DC_t = 3$ (M\$/m) is the deficit cost. Note that this is used only in evaluating the optimal solution by simulation and is not involved in the optimization models. We define the total cost after applying (31) and (32) as the “penalized cost.”

[57] To see the mean shortage in (MCM) units and not via penalty, the cost increment in Table 2 should be divided by the deficit cost. For example, the mean shortage associated with the NP is $(1074.89 - 984.54)/3 = 30.11$ (m) i.e., $30.11 \times 0.8 = 24$ (MCM).

[58] Figures 3 and 4 demonstrate the simulation results for NP and RP3: Where subfigures show the results for each sample: (1) the final water level in aquifer 1, (2) the final water level in aquifer 2, (3) the total operation cost, and (4) the penalized cost.

[59] The NP results in ~50% of the samples deviating from the operation limits at the final stage in both aquifers, while in RP3 there are only four deviations over all simulations. Figures 3d and 4d show that ~10% of the samples in the NP exceed the worst cost of RP3. Moreover, a very large difference in the cost variability is exposed.

[60] Table 2 reports the empirical maximum, minimum, average, and standard deviation of the total and penalized cost for each policy, along with the empirical reliability defined as the fraction of the total simulations which maintain feasibility in both aquifers in all years. The constant value of the cost standard deviation in Table 2 indicates that all policies run on the same sample of the recharge; this indicates that the results are obtained from a fair simulation experiment.

[61] The results show that the cost of the NP range between 916–1061 M\$ while the cost of the RP3 range between 1021–1166 M\$. The NP yields infeasible situations in 51.4% of the samples while the unreliability of RP3 is only 0.3%. The low cost of NP does not mean there is an

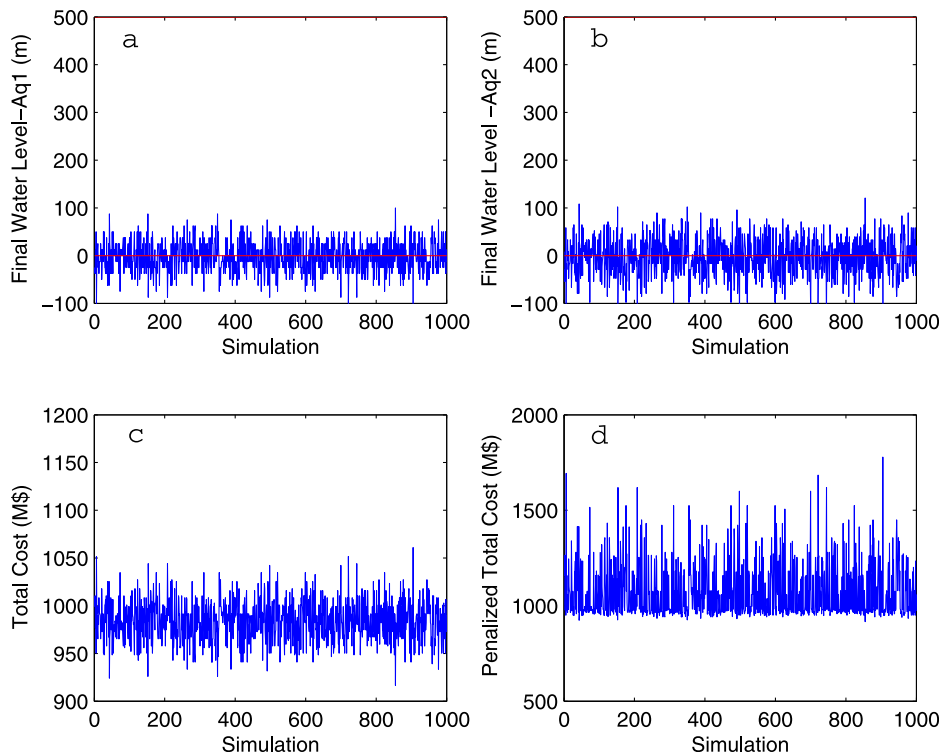


Figure 3. Simulation results of the NP.

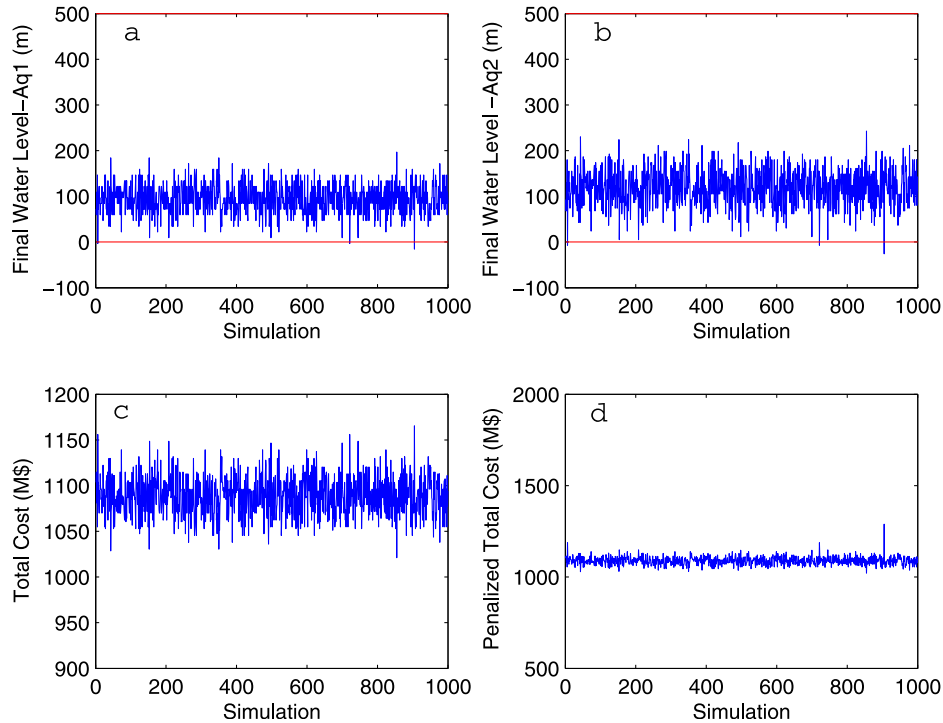


Figure 4. Simulation results of the RP3 policy.

advantage over RP3, since there is a very large difference in the reliabilities and it is a matter of multiobjective decision-making. Accounting for the constraints violation in the cost (Figures 3d and 4d) shows clear preference for RP3 over NP. RP3 immunizes the NP from a reliability of 48.6% to 99.7% with only a 10.6% increase in the mean cost. RP3 immunizes the NP with the price of robustness (mean cost increment) of 2.05 M\$ for each 1% reliability, while the CP immunizes it with price of robustness of 3.6 M\$ for each 1% reliability. Comparing CP with RP3 shows a clear preference of RP3; since the CP immunizes RP3 by getting rid of the last remaining 0.3% of unreliability with an associated cost of 80.5 M\$, or 268 M\$ for each 1% reliability.

[62] Figure 5 shows the tradeoff between reliability and mean cost for all policies. The tradeoff is characterized by a mild slope of the last segment connecting RP3 with CP, which indicates that a large increment in the mean cost is needed to obtain a small increment in reliability. The question to be asked is whether it is justified to add this large cost to immunize against rare events of the recharge. In our case the answer is given by the penalized cost which quantifies the unreliability by a penalty. The CP does not violate any constraint over all realizations of the recharge; hence,

the cost and penalized cost are identical. In Table 2 the mean penalized cost of RP3 is 80.34 M\$ less than the mean cost of CP, in contrast the CP maximum cost is 43.22 M\$ less than the maximum penalized cost of RP3. However, further analysis of the cost distribution shows that only one sample in RP3 would exceed the worst cost of the CP (1246 M\$) while 695 samples in RP3 are below the best cost of the CP (1101.6 M\$).

[63] This results shows that implementation of the CP would increase the mean cost by 80.34 M\$ while the only gain is reduction of 43.22 M\$ in the cost’s upper bound, which is rarely realized.

[64] Policies RP2 and RP3 are indeed robust, the corresponding standard deviations of the penalized cost are by a factor of 4.2–6.4 less than the NP standard deviation, indicating that these robust policies lead to stable policies without large variability in the associated costs, which can be accounted for as a preference over other alternatives.

5.3. Folding Robust Counterpart (FRC)

[65] The RC approach solves a static problem in which the decisions are “here and now” for all years, as if all future decisions are fixed in advance. This may seem like a

Table 2. Simulation Results for the Static Policies^a

| Policy | Cost (M\$) | | | | Penalized cost (M\$) | | | | Reliability (%) |
|--------|------------|---------|---------|-------|----------------------|---------|---------|--------|-----------------|
| | Min | Max | Mean | SD | Min | Max | Mean | SD | |
| NP | 916.60 | 1060.98 | 984.54 | 21.27 | 916.60 | 1778.32 | 1074.89 | 143.71 | 48.6 |
| RP1 | 948.43 | 1092.81 | 1016.38 | 21.27 | 948.43 | 1613.35 | 1035.52 | 74.01 | 81.4 |
| RP2 | 983.28 | 1127.66 | 1051.22 | 21.27 | 983.28 | 1451.40 | 1053.66 | 34.07 | 97.7 |
| RP3 | 1021.09 | 1165.46 | 1089.03 | 21.27 | 1021.09 | 1289.22 | 1089.22 | 22.29 | 99.7 |
| CP | 1101.62 | 1246.00 | 1169.56 | 21.27 | 1101.62 | 1246.00 | 1169.56 | 21.27 | 100 |

^aNP, Nominal Policy; RP1, Robust Policy $\theta = 1$; RP2, Robust Policy $\theta = 2$; RP3, Robust Policy $\theta = 3$; CP, Conservative Policy; M\$, Million \$; SD, Standard Deviation.

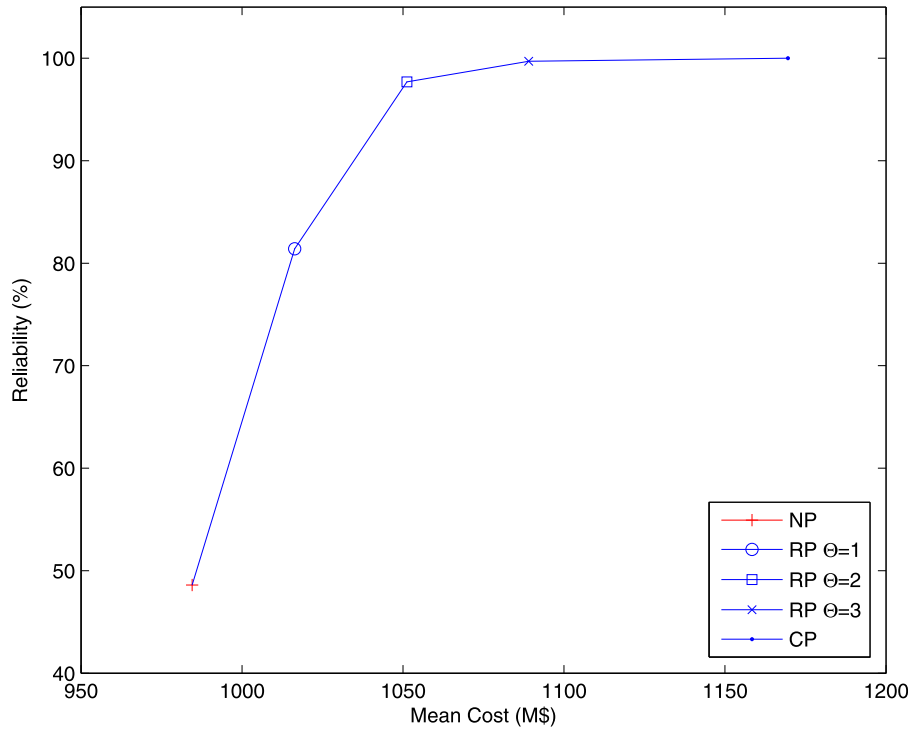


Figure 5. Reliability versus cost.

myopic approach, but in fact only the decision for the first year should be implemented and the analysis is then repeated toward the end of this year, with new information (if any) about the recharge, demands, costs, and initial system state (aquifer water levels). This is captured in the folding robust counterpart (FRC) model.

[66] At time “now,” the RC solution for all years is computed, and the first stage decision is implemented. At the beginning of the next year, we solve a new problem with a new state (obtained from the first year decision and realization) and reduced time horizon. This is repeated over all of the stages (years).

[67] We next demonstrate and compare the folding robust policy (FRP) with the folding multistage stochastic programming policy (FMSPP). The comparison is carried out for the small system in Figure 1 with the data listed earlier, where the aquifers recharge at each year is i.i.d. given by multivariate normal distribution with an expectation $\mu = [40, 48.33]$ and the covariance matrix V defined in (29).

5.3.1. Multistage Stochastic Programming (MSP)

[68] A well-studied method for solving multistage stochastic decision models is multistage stochastic programming [Shapiro *et al.*, 2009]. In the MSP we capture the uncertainty as a stochastic process with a known probability distribution. One variant of the MSP is scenarios-based, which assumes that the distribution of the stochastic process is given by a finite number of scenarios, each with its corresponding probability p^s . Following this approach, the stochastic recharge of the example in section 5.1 is modeled by a 10-stage scenario tree having three branches at each stage with identical probabilities. This scenario tree has 3^{10} different scenarios, which at each stage t are bundled into 3^t nodes while all scenarios which share the same node at stage t have the same recharge up to this stage.

[69] At any node in the multistage scenario tree, the decision-maker knows the exact history leading to that node, and decides how to proceed, knowing only that the future recharge is presented by each of the scenarios that emerge from the node into the future. The MSP solves for all stages simultaneously to obtain the optimal decisions (corresponding to each node) which results in a minimum expectation cost over all scenarios. The MSP model for the WSS model is

$$\begin{aligned}
 & \sum_{s=1}^{\text{Scenarios}} p^s K^s \rightarrow \min \\
 & \text{Subject to} \\
 & \sum_{t=1}^{T_f} \sum_a \frac{E_a Q_{a,t}^s}{SA_a} - \sum_{t=1}^{T_f} \sum_a \frac{E_a R_{a,t}^s}{SA_a} + \sum_{t=1}^{T_f} \sum_d des_{d,t} Q_{d,t}^s \\
 & \quad + \sum_{t=1}^{T_f} \sum_l C_{l,t} Q_{l,t}^s + P_0 - K^s \leq 0 \quad \forall s \\
 & h_{a,0} + \frac{1}{SA_a} \left(\sum_{i=1}^t R_{a,i}^s - \sum_{i=1}^t Q_{a,i}^s \right) - h_{a,t}^{\max} \leq 0 \quad \forall a \forall t \forall s \\
 & -h_{a,0} - \frac{1}{SA_a} \left(\sum_{i=1}^t R_{a,i}^s - \sum_{i=1}^t Q_{a,i}^s \right) + h_{a,t}^{\min} \leq 0 \quad \forall a \forall t \forall s \\
 & GQ_t^s = S_t \quad \forall t \forall s \\
 & Q_{d,t}^{\min} \leq Q_{d,t}^s \leq Q_{d,t}^{\max} \quad \forall d \forall t \forall s \\
 & 0 \leq Q_{a,t}^s \leq Q_{a,t}^{\max} \quad \forall a \forall t \forall s \\
 & 0 \leq Q_{l,t}^s \leq Q_{l,t}^{\max} \quad \forall l \forall t \forall s \\
 & Q_t^s \in \mathcal{N} \quad \forall t \forall s,
 \end{aligned} \tag{33}$$

where s denotes scenario; p^s is the probability associated with each scenario; \mathcal{N} is the set of nonanticipativity

Table 3. Discrete Approximation of the Multivariate Normal Distribution^a

| | | | | | |
|----------|--------------|--------------|-----------|--------------|--------------|
| Ra1, Ra2 | 23.67, 27.79 | 31.84, 38.06 | 40, 48.33 | 48.17, 58.61 | 56.33, 68.88 |
| Prob. | 0.06 | 0.22 | 0.44 | 0.22 | 0.06 |

^aRa1, Recharge in Aquifer 1; Ra2, Recharge in Aquifer 2; Prob., Probability.

constraints, which are the set of constraints such that $Q_t^{s_1} = Q_t^{s_2}$ for all scenarios s_1 and s_2 that are indistinguishable (share the same history) up to stage t [Shapiro et al., 2009, p. 71].

[70] In the general case of continuous distributed random data, the MSP is computationally intractable; however, we can apply the MSP by approximating the continuous distributions of the data by discrete ones. In our case the multivariate normal distribution is discretized. The size of the deterministic equivalent of the stochastic program depends on the number of elements considered in the discrete distribution. We chose a five-element discrete distribution $\{\mu, \mu \pm \sigma, \mu \pm 2\sigma\}$ given in Table 3 to represent the continuous normal distribution.

[71] With regard to the computational difficulty of solving the deterministic equivalent of the stochastic program, the nonanticipativity constraints can be eliminated by a substitution for the variables; this reduces the total number of constraints and variables in the problem. Still, the real computational difficulty arises due to the number of scenarios considered in the problem since the size of the deterministic program increases rapidly with the number of scenarios. For the example considered in section 5.1 with a 5-value distribution of the recharge as given in Table 3, the 10-stage problem would result in 36,621,091 variables and 141,601,544 inequality constraints even after elimination of the nonanticipativity constraints, while the RC of the 10-stage example has only 111 variables and 381 constraints. To reduce the computational burden for this presentation (since it is not the main purpose in this paper) we compare the performance of the three dynamic methods: FRP and FMSPP on a five-stage example in which the MSP results in 11,716 variables and 45,299 constraints while the RC results in 56 variables and 191 constraints.

5.3.2. Folding Horizon Simulation

[72] To evaluate these policies for the example outlined in section 5 with five-stages, we simulate their optimal solutions with 1000 random samples of $a_f T_f = 10$ random members each, drawn from the multivariate normal distribution of the recharge.

[73] The MSP is a sequential decision making approach; hence, it provides the optimal decision at each stage according to the history up to that stage. However, the MSP only

considered the discrete approximation of the continuous distribution. Hence, the MSP is also applied in the folding mode, since the realization of the recharge could be different from the values in the discrete approximation.

[74] To apply the folding horizon, for each sample we start by solving a five-stage problem. From the five-stage solutions we only adopt the first stage optimal solution according to each policy, i.e., RP and MSPP. Then we use the first member of the sample as if it is the actual realization of the recharge at the first stage. The new state of the system at the end of the first stage is calculated, given the decisions and the realization of the first stage.

[75] After this stage is fully covered, a four-stage problem is solved with the initial state corresponding to each of the states obtained at the end of the first stage. We continue with this procedure until we solve the problem of the fifth stage for all its possible initial states. At the end of the horizon we can calculate the total cost of each policy corresponding to the sample. Applying this procedure for each of the 1000 samples we obtain the simulation results for comparing the methods.

5.3.3. Simulation Results

[76] Table 4 reports the simulation results for the three dynamic decision-making policies: the static policy RP with $\theta = 3$, the FRP with $\theta = 3$, and FMSPP.

[77] Table 4 contains the maximum, minimum, average, and standard deviation of the total and the penalized cost for each policy, along with the empirical reliability defined as the fraction of the total simulations, which maintain feasibility in all aquifers and at all stages.

[78] The advantage of the adjustable dynamic RP over the static one is apparent. Both policies have a high reliability of 99.9%, but the dynamic policy results in a narrower and lower range of 301–569 M\$ instead of 393–604 M\$ and a lower mean cost of 418 M\$ compared to 451 M\$. The lower standard deviation of the static RP, is the result of the nonadjustability of the decision, namely in the folding mode the decisions depend on the realization and hence the standard deviation can be expected to increase.

[79] The FRP produces a more reliable solution than the FMSPP. The FRP immunizes the FMSPP with a price of robustness (mean cost increment) of 2.47 M\$ for each 1% reliability. Comparing the penalized cost, which quantifies the unreliability by the penalty, shows that the mean penalized cost of the FMSPP is 7.9 M\$ (1.9%) less than that obtained in the FRP; however, the worst and best cost of the FRP are less than in the FMSPP by 10.3% and 4.7%, respectively, and the standard deviation of the cost is smaller. Thus, in addition to better reliability, the FRP has greater flexibility to take advantage of opportunities (lower best cost) and to optimize in severe cases (lower worst cost).

Table 4. Simulation Results for the Dynamic Policies^a

| Policy | Cost (M\$) | | | | Penalized Cost (M\$) | | | | Reliability (%) |
|--------|------------|--------|--------|-------|----------------------|--------|--------|-------|-----------------|
| | Min | Max | Mean | SD | Min | Max | Mean | SD | |
| RP3 | 393.45 | 508.65 | 451.24 | 15.03 | 393.45 | 603.80 | 451.34 | 15.68 | 99.9 |
| FRP3 | 301.17 | 568.42 | 418.67 | 31.21 | 301.17 | 568.42 | 418.69 | 31.24 | 99.9 |
| FMSPP | 316.25 | 575.14 | 409.78 | 34.41 | 316.25 | 633.79 | 410.79 | 36.73 | 96.3 |

^aRP3, Robust Policy $\theta = 3$; FRP3, Folding RP3; FMSPP, Folding Multistage Stochastic Programming Policy; SD, Standard Deviation; M\$, Million \$.

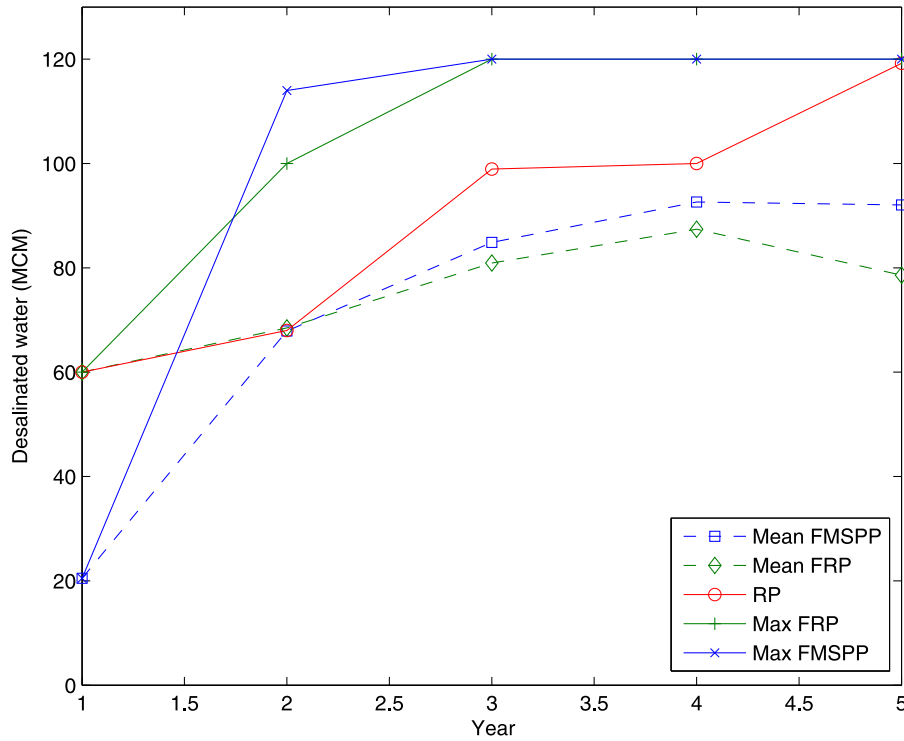


Figure 6. Desalination amount over years for each dynamic policy.

[80] The FRP solution could be a legitimate choice based on these results, but it is recommended that further statistical analysis of the penalized cost over longer periods and more simulations be required to determine preference. Still, the large size of the MSP model compared to the RP could tip the scales toward using the RP.

[81] The decisions in the folding mode are realization dependent, and hence each of decision variables starting from the second stage could take on as many values as the number of states obtained at the end of the previous stage.

[82] Figure 6 shows the maximum and mean desalination amount in each year according to each folding policy along with the desalination amount of the static policy (which is not realization dependent). The mean desalinated amount of the FRP is less than in the other policies, starting from the second year. The FMSP starts with low desalination, but soon after reaching the second stage fixes the desalination amount by a steep change to exceed the maximum desalination obtained from the FRP. However, both folding methods use the full capacity of the desalination plant starting from the third year.

5.4. Large System

[83] A water system shown in Figure 7 has nine demand zones, three aquifers, five desalination plants, and 49 pipes, and approximates the central part of the Israeli National Water System. The data for the model, including the recharge series, are presented as supplementary material.¹ The full recharge record of the three aquifers has 78 annual values (1932–2009, Israeli Hydrological Service). We demonstrate the RC approach based on part of this historical

¹Auxiliary materials are available at <ftp://ftp.agu.org/apend/journal/2011WR010596>.

record (1932–2004) and then simulate the RC approach in folding mode to imitate the adoption of a folding robust policy (FRP) in 2005. The results are also compared to the folding nominal policy (FNP).

[84] The ellipsoidal uncertainty set for the RC model is based on the computed means and covariance matrix of the recharge into the three aquifers:

$$\mu_{R'} = \begin{pmatrix} 210 \\ 100 \\ 81 \end{pmatrix}, \quad V_{R'} = \begin{pmatrix} 3702 & 1585 & 4576 \\ 1585 & 1255 & 3428 \\ 4576 & 3428 & 9813 \end{pmatrix}. \quad (34)$$

[85] According to section 4.1, the uncertainty set of the annual recharge is

$$U = \left\{ R' : \begin{pmatrix} 210 \\ 100 \\ 281 \end{pmatrix} + \begin{pmatrix} 60.84 & 0 & 0 \\ 26.05 & 24 & 0 \\ 75.2 & 61.17 & 20.34 \end{pmatrix} \begin{pmatrix} s_1 \\ s_2 \\ s_3 \end{pmatrix}, \|s\| \leq \theta \right\}. \quad (35)$$

[86] Figure 8 shows the water level of the three aquifers according to each of the two policies. In aquifer 1 the FRP raises the water level by an almost constant increment each year. In aquifer 3 the gap between the water level obtained by the FRP and the one from FNP increases over time to such an extent that the water level of the FNP is below the minimum water level allowed.

[87] In aquifer 2, both policies result in the same water level over years; this is because of the limitation of the network topology associated with this aquifer, as can be seen in Figure 7 where aquifer 2 can supply only to demand zone 2.

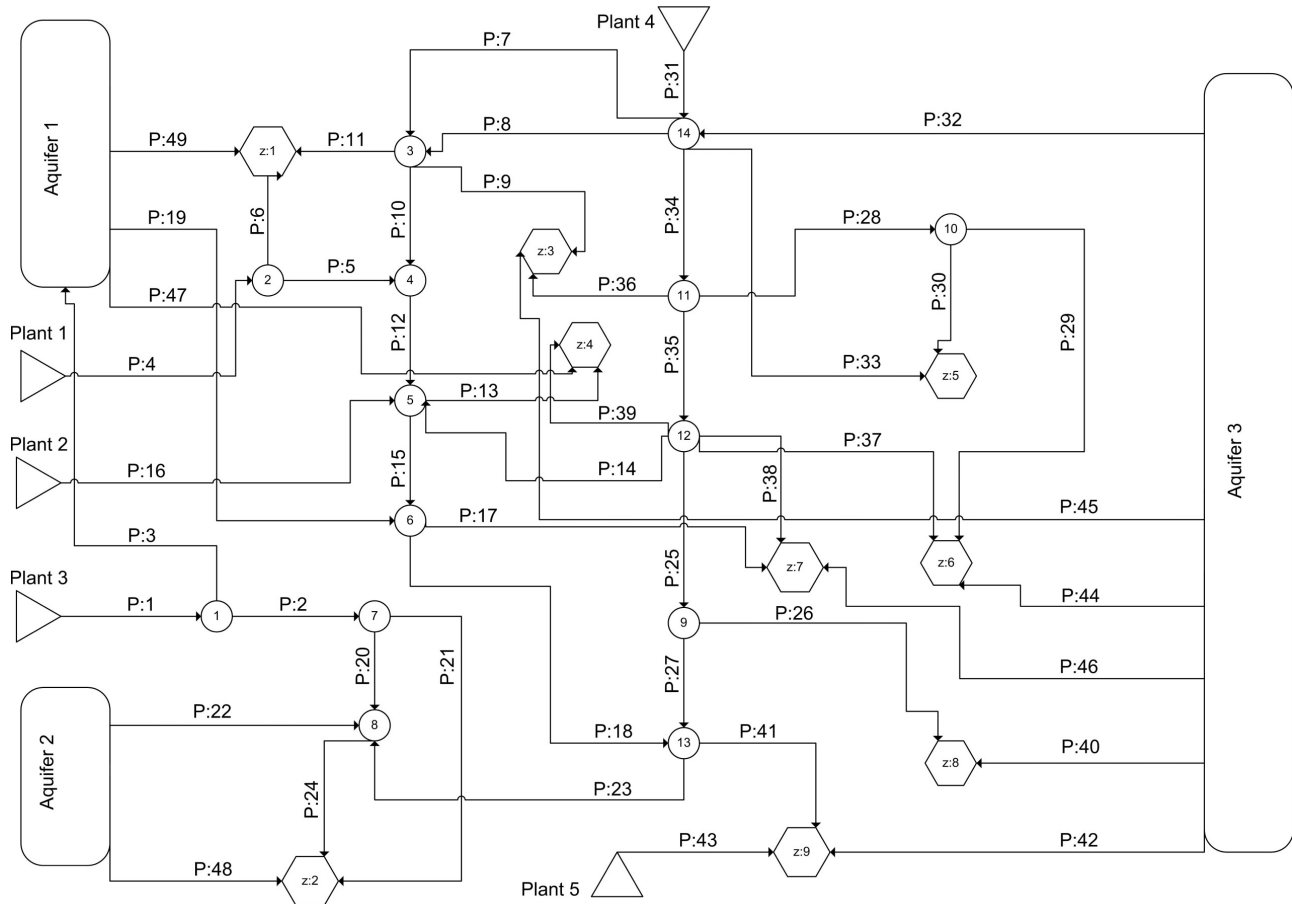


Figure 7. Network layout of the large system.

6. Conclusions

[88] The underlying concepts of the RC method show considerable promise, regarding the tractability of the models and the results obtained. The results demonstrate the advantage of being able to replace the stochastic behavior of the uncertainty by specifying a user-defined set within which the resulting policies are immunized (remain feasible), as well as being able to show the trade-off between reliability and cost.

[89] The method and its dynamic variant folding RC were applied to a small WSS as a test bed, and to a central part of the Israeli National Water System. The results are very competitive with those obtained by stochastic and deterministic methods. While the advantage of the RP over the NP and CP is apparent as demonstrated in section 5.2., the advantage over the multistage stochastic programming is not. On the one hand, the FRP obtains better reliability and has greater flexibility to take advantage of opportunities (lower best cost) and to optimize severe cases (lower worst cost). On the other hand, the stochastic programming solution has a lower mean cost.

[90] The small size of the RP model compared to the MSP is a remarkable advantage of the robust optimization method. The RC approach presented in this paper is inherently static by design; to capture the dynamic nature of the problem we applied the RC in a folding mode. We continue

to develop and test a variety of robust optimization based methods [Ben-Tal et al., 2009], including the adjustable robust counterpart (ARC) and the affine adjustable robust counterpart (AARC) which are inherently dynamic by design.

[91] A drawback of the presented model is the absence of nonlinear processes, such as those that appear when water salinity is considered. We propose some research directions for the incorporation of nonlinearity with the RO methodology: (1) Nonlinear convex functions could be approximated by a convex piecewise linear functions. Thus, for cost minimization the model can be reformulated as a linear program. (2) Incorporating salinity in the model introduces bi-linear relations, which can be handled in two inter-related iterative steps: (1) fixing the salinity variables makes the problem linear with respect to the flows, and (2) fixing the flows makes the problem linear with respect to the salinities. This decomposition facilitates the application of the RC: the flow variables and the salinity variables are solved separately and coordinated iteratively. (3) The nonlinear RC model can be solved by a sequential linear programming (SLP) algorithm. The SLP consists of linearizing the objective and constraints in a region around a nominal operating point by a Taylor series expansion. The resulting linear programming problem is then solved by the RC approach.

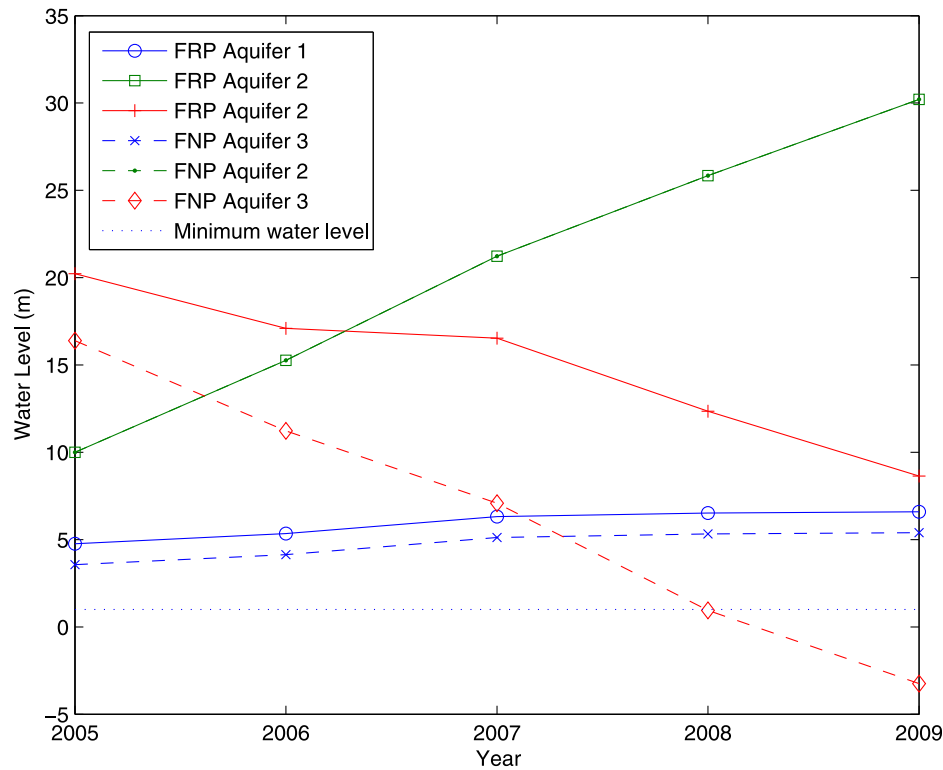


Figure 8. Aquifers water levels in the large system.

[92] **Acknowledgments.** Financial support of the first author by the Technion - Israel Institute of Technology is gratefully acknowledged. We are indebted to Aharon Ben-Tal (Technion) for advice on the method, and to Miki Zaide (Strategic Planner, Israeli Water Authority) for providing the data on the Israeli National Water System.

References

- Ajami, N. K., G. M. Hornberger, and D. L. Sunding (2008), Sustainable water resource management under hydrological uncertainty, *Water Resour. Res.*, 44(11), W11406, doi:10.1029/2007WR006736.
- Ben-Tal, A., and A. Nemirovski (1998), Robust convex optimization, *Math. Oper. Res.*, 23(4), 769–805.
- Ben-Tal, A., and A. Nemirovski (1999), Robust solutions to uncertain linear programs, *Oper. Res. Lett.*, 25, 1–13.
- Ben-Tal, A., and A. Nemirovski (2000a), Robust solutions of linear programming problems contaminated with uncertain data, *Math. Program.*, 88, 411–421.
- Ben-Tal, A., T. Margalit, and A. Nemirovski (2000b), Robust modeling of multi-stage portfolio problems, in *High Performance Optimization*, edited by H. Frank, et al., chpt. 12, pp. 303–328, Kluwer Acad., Rotterdam, Netherlands.
- Ben-Tal, A., L. El Ghaoui, and A. Nemirovski (2009), *Robust Optimization*, 564 pp., Princeton Univ. Press, N. J.
- Bertsimas, D., and A. Thiele (2006), A robust optimization approach to supply chain management, *Oper. Res.*, 54(1), 150–168.
- Bertsimas, D., and M. Sim (2004), The price of robustness, *Oper. Res.*, 52(1), 35–53.
- Bienstock, D., and N. Ozbay (2008), Computing robust base stock levels, *Discrete Optimization*, 5(2), 389–414.
- Brekke, L. D., E. P. Maurer, J. D. Anderson, M. D. Dettinger, E. S. Townsley, A. Harrison, and T. Pruitt (2009), Assessing reservoir operations risk under climate change, *Water Resour. Res.*, 45(4), W04411, doi:10.1029/2008WR006941.
- Chung, G., K. Lansey, and G. Bayraksan (2009), Reliable water supply system design under uncertainty, *Environ. Modell. Software*, 24, 449–462.
- Cohen, D., U. Shamir, and G. Sinai (2000), Optimal operation of multi-quality water supply systems-I: Introduction and the Q-C model, *Eng. Optimization*, 32(5), 549–584.
- Draper, A. J., M. W. Jenkins, K. W. Kirby, J. R. Lund, and R. E. Howitt (2003), Economic-engineering optimization for California water management, *J. Water Resour. Plann. Manage.*, 129(3), 155–164.
- Draper, A. J., A. Munévar, S. K. Arora, E. Reyes, N. L. Parker, F. I. Chung, and L. E. Peterson (2004), CalSim: Generalized model for reservoir system analysis, *J. Water Resour. Plann. Manage.*, 130(6), 480–489.
- Escudero, L. F. (2000), WARSYP: A robust modeling approach for water resources system planning under uncertainty, *Annals of Operations Research*, 95, 313–339.
- Faber, B. A., and J. R. Stedinger (2001), Reservoir optimization using sampling SDP with ensemble stream flow prediction forecasts, *J. Hydrol.*, 249(1–4), 113–133.
- Fisher, F. M., S. Arlosoroff, Z. Eckstein, M. Haddadin, S. G. Hamati, A. Huber-Lee, A. Jarrar, A. Jauouosi, U. Shamir, and H. Wesseling (2002), Optimal water management and conflict resolution: The Middle East water project, *Water Resour. Res.*, 38(11), 251–2517, 1243, doi:10.1029/2001WR000943.
- Jenkins, M. W., J. R. Lund, R. E. Howitt, A. J. Draper, S. M. Msangi, S. K. Tanaka, R. S. Ritzema, and G. F. Marques (2004), Optimization of California's water supply system: Results and insights, *J. Water Resour. Plann. Manage.*, 130(4), 271–280.
- Jia, Y. B., and T. B. Culver (2006), Robust optimization for total maximum daily load allocations, *Water Resour. Res.*, 42(2), W02412, doi:10.1029/2005WR004079.
- Kasprzyk, J. R., P. M. Reed, B. R. Kirsch, and G. W. Characklis (2009), Managing population and drought risks using many-objective water portfolio planning under uncertainty, *Water Resour. Res.*, 45(12), W12401, doi:10.1029/2009WR008121.
- Kracman, D. R., D. C. McKinney, D. W. Watkins Jr., and L. S. Lasdon (2006), Stochastic optimization of the highland lakes system in Texas, *J. Water Resour. Plann. Manage.*, 132(2), 62–70.
- Labadie, J. W. (2004), Optimal operation of multi-reservoir systems: State-of-the-art review, *J. Water Resour. Plann. Manage.*, 130(2), 93–111.
- Lansey, K. E., N. Duan, L. W. Mays, and Y. K. Tung (1989), Water distribution system design under uncertainties, *J. Water Resour. Plann. Manage.*, 115(5), 630–645.
- Li, Z., and M. G. Ierapetritou (2008), Robust optimization for process scheduling under uncertainty, *Ind. Eng. Chem. Res.*, 47, 4148–4157.

- Lobo, M. S., and S. Boyd (2000), The worst-case risk of a portfolio, *Tech. Rep.* (available at http://www.stanford.edu/~boyd/papers/pdf/risk_bnd.pdf)
- Loucks, D. P. (2000), Sustainable water resources management, *Water Int.*, 25(1), 3–10.
- Loucks, D. P., J. R. Stedinger, and D. A. Haith (1981), Water resource systems planning and analysis, 559 pp., *Prentice Hall*, Englewood Cliffs, N. J.
- Lund, J. R., and I. Ferreira (1996), Operating rule optimization for Missouri river reservoir system, *J. Water Resour. Plann. Manage.*, 122(4), 287–295.
- Mudchanatongsuk, S., F. Ordóñez, and J. Zhao (2005), Robust solutions for network design under transportation cost and demand uncertainty, *J. Oper. Res. Soc.*, 59, 652–662.
- Mulvey, J. M., R. J. Vanderbei, and S. A. Zenios (1995), Robust optimization of large-scale systems, *Oper. Res.*, 43(2), 264–281.
- Ostfeld, A., and U. Shamir (1993), Optimal operation of multi-quality networks. I: Steady-state conditions, *J. Water Resour. Plann. Manage.*, 119(6), 645–662.
- Pallottino, S., G. M. Sechi, and P. Zuddas (2005), A DSS for water resources management under uncertainty by scenario analysis, *Environ. Modell. Software*, 20(8), 1031–1042.
- Sankarasubramanian, A., U. Lall, F. Souza, A. Filho, and A. Sharma (2009), Improved water allocation utilizing probabilistic climate forecasts: Short-term water contracts in a risk management framework, *Water Resour. Res.*, 45, W11409, doi:10.1029/2009WR007821.
- Sen, S., and J. L. Hight (1999), An introductory tutorial on stochastic linear programming models, *Interfaces*, 29(2), 33–61.
- Shamir, U. (1971), A Hierarchy of Models for Optimizing the Operation of Water Systems, *Symposium on The Water Environment and Human Needs*, edited by A. T. Ippen, pp. 284–301, MIT Press, Mass.
- Shapiro, A., D. Dentcheva, and A. Ruszczyński (2009), *Lectures on Stochastic Programming: Modeling and Theory*, 447 pp., SIAM, Philadelphia, Pa.
- Soyster, A. L. (1973), Convex programming with set-inclusive constraints and applications to inexact linear programming, *Oper. Res.*, 21, 1154–1157.
- Watkins, D. W., and D. C. McKinney (1997), Finding robust solutions to water resources problems, *J. Water Resour. Plann. Manage.*, 123(1), 49–58.
- Watkins, D. W., Jr., K. W. Kirby, and R. E. Punnett (2004), Water for the everglades: Application of the South Florida systems analysis model, *J. Water Resour. Plann. Manage.*, 130(5), 359–366.
- Yates, D., D. Purkey, J. Sieber, A. Huber-Lee, and H. Galbraith (2005), WEAP21—A demand priority and preference-driven water planning model. Part 2: Aiding freshwater ecosystem service evaluation, *Water Int.*, 30(4), 501–512.
- Yeh, W. (1985), Reservoir management and operations models: A state-of-the-art review, *Water Resour. Res.*, 21(12), 1797–1818, doi:10.1029/WR021i012p01797.
- Zaide, M. (2006), A model for multiyear combined optimal management of quantity and quality in the Israeli national water supply system, *M.Sc thesis*, Technion—I.I.T., available at <http://urishamir.wri.technion.ac.il/files/documents/Miki%20Zaide%20-%20Thesis%20Final%2015.03.06.pdf> (accessed July 28, 2011).

M. Housh, A. Ostfeld, and U. Shamir, Faculty of Civil and Environmental Engineering, Technion, Israel Institute of Technology, Haifa 32000, Israel. (mashor@technion.ac.il)